Title: Complex critical points and curved geometries in four-dimensional Lorentzian spinfoam quantum gravity

Speakers: Dongxue Qu

Series: Quantum Gravity

Date: November 24, 2021 - 4:00 PM

URL: https://pirsa.org/21110039

Abstract: This talk focuses on the semiclassical behavior of the spinfoam quantum gravity in 4 dimensions. There has been long-standing confusion, known as the flatness problem, about whether the curved geometry exists in the semiclassical regime of the spinfoam amplitude. The confusion is resolved by the present work. By numerical computations, we explicitly find curved Regge geometries from the large-j Lorentzian Engle-Pereira-Rovelli-Livine (EPRL) spinfoam amplitudes on triangulations. These curved geometries are with small deficit angles and relate to the complex critical points of the amplitude. The dominant contribution from the curved geometry to the spinfoam amplitude is proportional to e^{i I}, where I is the Regge action of the geometry plus corrections of higher order in curvature. As a result, the spinfoam amplitude reduces to an integral over Regge geometries weighted by e^{i I} in the semiclassical regime. As a byproduct, our result also provides a mechanism to relax the cosine problem in the spinfoam model. Our results provide important evidence supporting the semiclassical consistency of the spinfoam quantum gravity.

Zoom Link: https://pitp.zoom.us/j/93699343757?pwd=RnpFeitaTU5qTktzNjlXQW45K1gvQT09

Complex critical points and curved geometries in Lorentzian EPRL spinfoam amplitude

Dongxue Qu

Florida Atlantic University

Collaborators: Muxin Han, Zichang Huang and Hongguang Liu

Preprint: arXiv:2110.10670

Nov. 24th, 2021 @ PI

Outline

Go to page 12

Motivation and Results

- The semiclassical consistency is an important requirement in LQG.
- We focus on 4-dimensional Lorentzian EPRL spinfoam formulation.
- Semiclassical approximation $\Longrightarrow$ Large-j asymptotics of spinfoam amplitude.

  [Asante, Bahr, Barrett, Bianchi, Bonzom, Conrady, Ding, Dittrich, Dona, Engle, Freidel, Gozzini, Haggard, Han, Hellmann, Huang, Kaminski, Kisielowski, Liu, Livine, Magliaro, Perini, Pereira, Riello, Rovelli, Sahlmann, Sarno, Speziale, Zhang, etc.]
- Asymtotics of the spinfoam amplitude relates to Regge calculus
- Recent progress in numerics on spinfoam models
  - sl2cfoam based on $15j$ + boosters [Dona, Fanizza, Sarno, Speziale, Gozzini 2018-2021]
  - Spinfoam renormalization [Bahr, Dittrich, Steinhaus, 2016-2021]
  - Effective spinfoam model [Asante, Dittrich, Haggard, 2020-2021]
  - Asymptotics expansion, Lefschetz thimble, Monte-Carlo [Han, Huang, Liu, DQ, 2020-2021]
- Simplicial complex, sum over j $\rightarrow$ Flatness problem:

The EPRL spinfoam amplitude seems to be dominated *only* by flat Regge geometries in the semiclassical regime.

The numerics demonstrates curved geometries whose contributions are not small in EPRL spinfoam amplitudes.

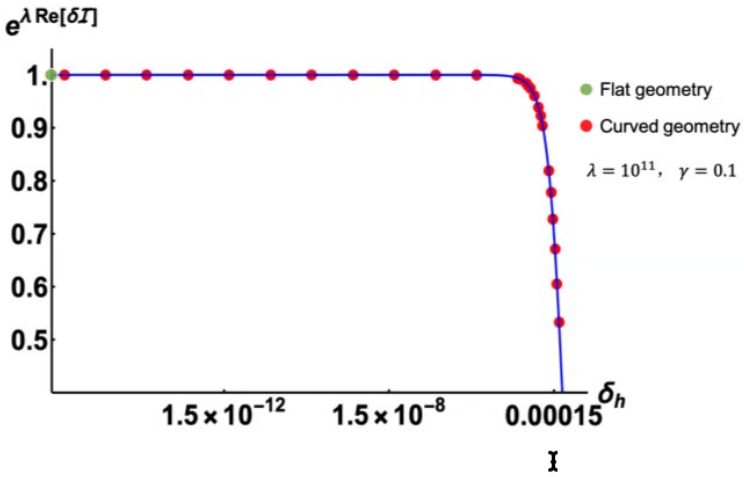

Horizontal axis: deficit angle δ_h; Vertical axis: $\propto$ Amplitudes

Similar ideas appeared in

[Asante, Dittrich, Haggard, 2020]

[Han, 2013]

[Engle, Kaminski, Oliveira 2020]

In spinfoam, large spin parameter λ is a *finite* expansion parameter.

For any large but finite λ, there exists relatively small deficit angles such that the amplitude is not small.

$\gamma = 0.1$

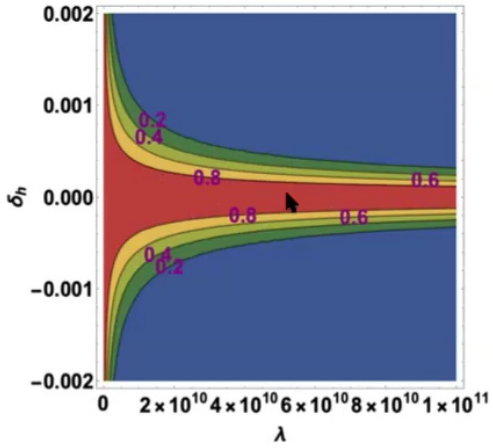

$\lambda = 5 \times 10^{10}$

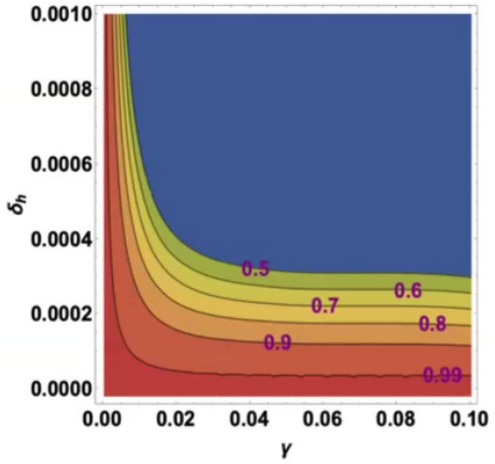

The non-blue regime of curved geometries where the amplitude is not small.

Effective action: Regge action plus "high curvature correction"

$$\mathcal{S} = i\mathcal{I}_R[\mathbf{g}(r)] + a_2\delta_h^2 + a_3\delta_h^3 + a_4\delta_h^4 + O(\delta_h^5),$$

- These curved geometries come from complex critical points.
- A warm-up example

$$A_\lambda(r) = \int_{-\infty}^{+\infty} e^{\lambda\left[ix^2 - r(x+1)^2\right]} dx, \quad r \geq 0, \quad \lambda \gg 1$$

The critical point: $x_c = \frac{r}{r-i} \begin{cases} r = 0 & \text{real critical point} \\ r \neq 0 & \text{complex critical point} \end{cases}$,

$$A_\lambda(r) = \frac{\sqrt{\pi}}{\sqrt{\lambda(r-i)}} e^{\lambda\left[ix_c^2 - r(x_c+1)^2\right]},$$

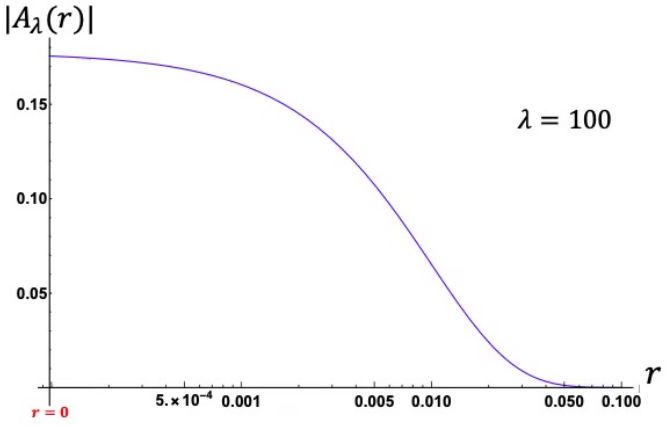

$\lambda = 100$

Similar ideas appeared in

[Asante, Dittrich, Haggard, 2020]

[Han, 2013]

[Engle, Kaminski, Oliveira 2020]

$\gamma = 0.1$

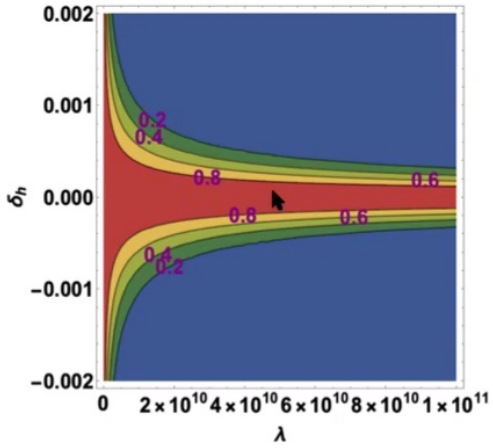

$\lambda = 5 \times 10^{10}$

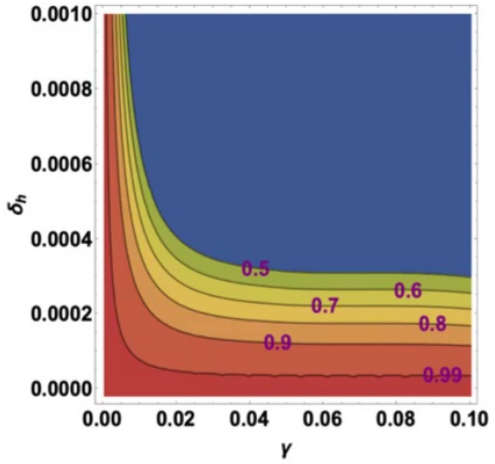

The non-blue regime of curved geometries where the amplitude is not small.

Effective action: Regge action plus "high curvature correction"

$$\mathcal{S} = i\mathcal{I}_R[\mathbf{g}(r)] + a_2\delta_h^2 + a_3\delta_h^3 + a_4\delta_h^4 + O(\delta_h^5),$$

- These curved geometries come from complex critical points.
- A warm-up example

$$A_\lambda(r) = \int_{-\infty}^{+\infty} e^{\lambda\left[ix^2 - r(x+1)^2\right]} dx, \quad r \geq 0, \quad \lambda \gg 1$$

The critical point: $x_c = \frac{r}{r-i} \begin{cases} r = 0 & \text{real critical point} \\ r \neq 0 & \text{complex critical point} \end{cases}$,

$$A_\lambda(r) = \frac{\sqrt{\pi}}{\sqrt{\lambda(r-i)}} e^{\lambda\left[ix_c^2 - r(x_c+1)^2\right]},$$

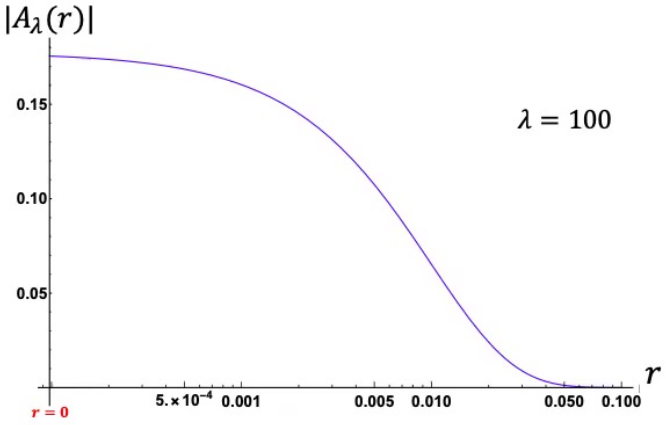

$\lambda = 100$

Similar ideas appeared in

[Asante, Dittrich, Haggard, 2020]

[Han, 2013]

[Engle, Kaminski, Oliveira 2020]

Motivation and Results

- Δ_3: relaxing cosine problem.
- 1-5 Pachner move: reduce the spinfoam amplitude to integral over Regge geometries:

$$\left(\frac{1}{\lambda}\right)^{\frac{N}{2}} \int \prod_{m=1}^{5} \mathrm{d}l_{m6}\, e^{\lambda \mathcal{S}(r,Z(r))} \mathscr{N}_r \left[1 + O(1/\lambda)\right],$$

Effective action $\mathcal{S}$ is Regge action plus "high curvature correction".

Outline

EPRL Spinfoam Model

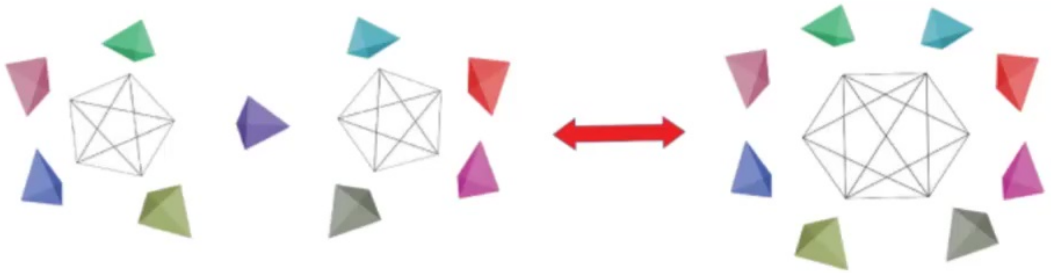

4-d triangulation $\mathcal{K}$

- 4-simplices: σ
- tetrahedra: τ
- triangles: t

dual complex $\mathcal{K}^*$

- vertices: v
- oriented edges: e
- oriented faces: f : h (internal), b (boundary)

A spinfoam assigns an SU(2) spin j_f to each face f: j_h, j_b.

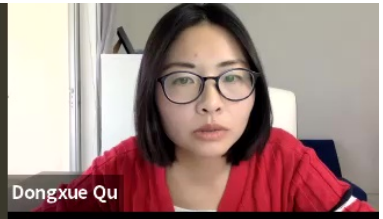

EPRL Spinfoam Amplitude

The spinfoam amplitude in the integral representation:

$$A(\mathcal{K}) = \sum_{\{j_h\}} \prod_h d_{j_h} \int [\mathrm{d}g_f \mathrm{d}\mathbf{z}]\, e^{S(j_h, g_{ve}, \mathbf{z}_{vf}; j_b, \xi_{eb})},$$

$$[\mathrm{d}g\mathrm{d}\mathbf{z}] = \prod_{(v,e)} \mathrm{d}g_{ve} \prod_{(v,f)} \mathrm{d}\Omega_{\mathbf{z}_{vf}},$$

- $|j_b, \xi_{eb}\rangle$: SU(2) boundary coherent state.
- $\mathbf{z}_{vf} \in \mathbb{CP}^1$.
- $g_{ve} \in \mathrm{SL}(2,\mathbb{C})$.
- phase amplitude $d_{j_h} = 2j_h + 1$.
- dg_{ve} is the Haar measure, $\mathrm{d}\Omega_{\mathbf{z}_{vf}}$ is a scaling invariant measure on $\mathbb{CP}^1$.

EPRL spinfoam action

The spinfoam action S is given by

$$
\begin{aligned}
S &= \sum_{(e',x)} j_h F_{(e',x)} + \sum_{(e,b)} j_b F_{(e,b)} + \sum_{(e',b)} j_b F_{(e',b)}, \\
F_{(e,b)} &= 2\ln \frac{\langle Z_{veb}, \xi_{eb}\rangle}{\|Z_{veb}\|} + i\gamma \ln \|Z_{veb}\|^2, \quad Z_{vef} = g_{ve}^{\dagger}\mathbf{z}_{vf} \\
&\text{or} \quad 2\ln \frac{\langle \xi_{eb}, Z_{v'eb}\rangle}{\|Z_{v'eb}\|} - i\gamma \ln \|Z_{v'eb}\|^2, \\
F_{(e',f)} &= 2\ln \frac{\langle Z_{ve'f}, Z_{v'e'f}\rangle}{\|Z_{ve'f}\|\,\|Z_{v'e'f}\|} + i\gamma \ln \frac{\|Z_{ve'f}\|^2}{\|Z_{v'e'f}\|^2},
\end{aligned}
$$

Continuous gauge freedom and gauge fixing:

- For each $\mathbf{z}_{vf}$, $\mathbf{z}_{vf} \mapsto \lambda_{vf}\mathbf{z}_{vf}$, $\lambda_{vf} \in \mathbb{C} \Longrightarrow \mathbf{z}_{vf} = (1, \alpha_{vf})^T$.
- At each v, $g_{ve} \mapsto x_v^{-1} g_{ve}$, $\mathbf{z}_{vf} \mapsto x_v^{\dagger}\mathbf{z}_{vf}$, $x_v \in \mathrm{SL}(2,\mathbb{C}) \Longrightarrow$ one $g_{ve} = 1$
- At each e, $g_{v'e} \mapsto g_{v'e}h_e^{-1}$, $g_{ve} \mapsto g_{ve}h_e^{-1}$, $h_e \in \mathrm{SU}(2) \Longrightarrow g_{v'e}$ to be upper-triangular matrix.

  (any $g \in \mathrm{SL}(2,\mathbb{C})$ can be written as $g = kh$ where k is upper-triangular and $h \in \mathrm{SU}(2)$).

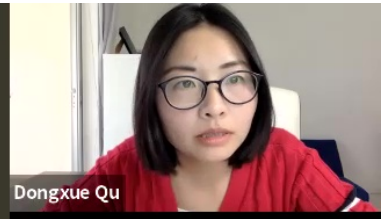

Real parametrization:

$$
\begin{aligned}
g_{v'e} &= \mathring{g}_{v'e} \begin{pmatrix} 1+\frac{x^1_{v'e}}{\sqrt{2}} & \frac{x^2_{v'e}+iy^2_{v'e}}{\sqrt{2}} \\ 0 & \mu_{v'e} \end{pmatrix} \in \mathrm{SL}(2,\mathbb{C}), \\
g_{ve} &= \mathring{g}_{ve} \begin{pmatrix} 1+\frac{x^1_{ve}+iy^1_{ve}}{\sqrt{2}} & \frac{x^2_{ve}+iy^2_{ve}}{\sqrt{2}} \\ \frac{x^3_{ve}+iy^3_{ve}}{\sqrt{2}} & \mu_{ve} \end{pmatrix} \in \mathrm{SL}(2,\mathbb{C}) \\
\mathbf{z}_{vf} &= (1, \mathring{\alpha}_{vf} + x_{vf} + iy_{vf}) \in \mathbb{CP}^1.
\end{aligned}
$$

- $x_{ve}, y_{ve}, x_{vf}, y_{vf}$ are real numbers.
- $\mathring{g} \in \mathrm{SL}(2,\mathbb{C})$ and $\mathring{\alpha} \in \mathbb{C}$ will be a critical point of S.

Therefore,

$$S\left(j_h, g_{ve}, \mathbf{z}_{vf}\right) = S(j_h, x_{ve}, y_{ve}, x_{vf}, y_{vf})$$

will be analytic continued (locally) to the holomorphic function

$$\mathcal{S}(j_h, x_{ve}, y_{ve}, x_{vf}, y_{vf}), \quad j_h, x_{ve}, y_{ve}, x_{vf}, y_{vf} \in \mathbb{C}$$

EPRL Spinfoam Amplitude

LQG area spectrum: $\mathfrak{a} = 8\pi\gamma\ell_p^2\sqrt{j(j+1)}, \quad \mathfrak{a} \gg \ell_p^2 \Longleftrightarrow j \gg 1$

Semiclassical regime $\Longleftrightarrow$ large-j regime.

To probe the semiclassical regime, we scale both boundary and internal spins

$$j_b \to \lambda j_b, \quad j_h \to \lambda j_h, \quad \lambda \gg 1$$

Apply the Poisson summation to the EPRL spinfoam amplitude:

$$\begin{aligned} A(\mathcal{K}) &= \sum_{\{k_h \in \mathbb{Z}\}} \int_{\mathbb{R}} \prod_h \mathrm{d}j_h \prod_h 2\lambda\, d_{\lambda j_h} \int [\mathrm{d}g\mathrm{d}\mathbf{z}]\, e^{\lambda S^{(k)}}, \\ S^{(k)} &= S + 4\pi i \sum_h j_h k_h, \end{aligned}$$

j_h is continuous.

Real Critical Points

- The integral in the spinfoam amplitude has the following form:

$$\int \mathrm{d}^N x\, \mu(x)\, e^{\lambda S(r,x)}, \quad \lambda \gg 1,$$

where r is boundary data, x is integration variable.

$$r = (j_b, \xi_{eb}), \quad x = \{j_h, x_{ve}, y_{ve}, x_{vf}, y_{vf}\} \in \mathbb{R}^N$$

- *Real critical point* $\mathring{x}$ is the solution of the critical equations

$$\mathrm{Re}(S(\mathring{x})) = \partial_x S(\mathring{x}) = 0,$$

- The solution gives Regge geometries subject to the flatness constraint (up to some "parity flips"):

$$\gamma\delta_h = \mathring{\theta} \mod 4\pi\mathbb{Z}.$$

- Spinfoam amplitudes seem to be dominated *only* by flat Regge geometries in the semiclassical regime.

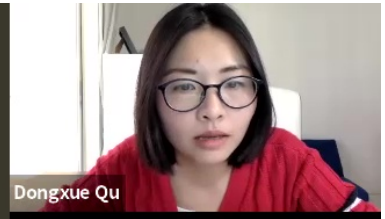

Δ_3 triangulation

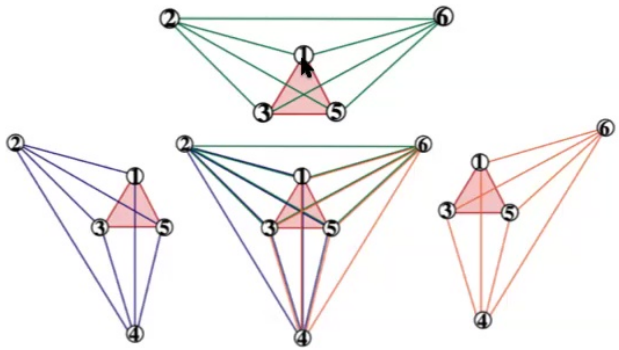

[Banburski, Chen, Freidel, Hnybida, 2015; Dona, Gozzini, Sarno, 2020; Asante, Dittrich, Haggard, 2020; Engle, Kaminski, Oliveira, 2020]

- Δ_3 contains three 4-simplices and a single internal face h.
- All edges are on the boundary, boundary edge-lengths determine Regge geometry on Δ_3.
- $r = \{j_b, \xi_{eb}\}$ is the boundary data, determining boundary edge-lengths, and Regge geometry $\mathbf{g}(r)$.
- All tetrahedra and triangles are spacelike.

Flatness Problem

- Regime 1: fixing the boundary data r admits a flat geometry on the triangulation

$$\int \mathrm{d}^N x\, \mu(x)\, e^{\lambda S(r,x)} = \left(\frac{1}{\lambda}\right)^{\frac{N}{2}} \frac{e^{\lambda S(r,\mathring{x})}\mu(\mathring{x})}{\sqrt{\det\left(-\delta^2_{x,x} S(r,\mathring{x})/2\pi\right)}} \left[1 + O(1/\lambda)\right]. \qquad (1)$$

The dominant contribution comes from the real critical point.

Flatness Problem

- Regime 1: fixing the boundary data r admits a flat geometry on the triangulation

$$\int \mathrm{d}^N x\, \mu(x)\, e^{\lambda S(r,x)} = \left(\frac{1}{\lambda}\right)^{\frac{N}{2}} \frac{e^{\lambda S(r,\mathring{x})}\mu(\mathring{x})}{\sqrt{\det\left(-\delta^2_{x,x} S(r,\mathring{x})/2\pi\right)}} \left[1 + O(1/\lambda)\right]. \qquad (1)$$

  The dominant contribution comes from the real critical point.

- Regime 2: fixing the boundary data r only admits the curved geometry, no real critical point, the amplitude is suppressed:

$$\int \mathrm{d}^N x\, \mu(x)\, e^{\lambda S(\mathbf{r},x)} = O(\lambda^{-K}), \quad \forall\, K > 0. \qquad (2)$$

- We also let r vary, then we need an interpolation between two regimes (1) and (2) in order to clarify contributions from curved geometries $\longrightarrow$ the use of *complex critical point*.

Complex Critical Points

We consider the large-λ integral:

$$\int_K \mathrm{d}^N x\, \mu(x)\, e^{\lambda S(r,x)}, \quad N = 124 \text{ for } \Delta_3,$$

- $S(r,x)$ and $\mu(x)$ are analytic functions for $r \in U \subset \mathbb{R}^k, x \in K \subset \mathbb{R}^N$.
- $U \times K$ is a compact neighborhood of $(\mathring{r}, \mathring{x})$.

Analytic Extension

$$x \to z \in \mathbb{C}^N, \quad S(r,x) \to \mathcal{S}(r,z)$$

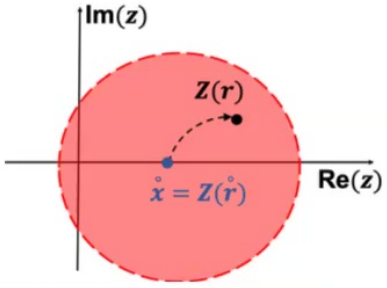

Complex critical points $z = Z(r)$ are the solutions of the complex critical equation

$$\partial_z \mathcal{S} = 0$$

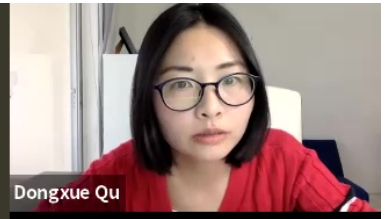

Complex Critical Points

[Hörmander, 1983; Melin, Sjöstrand, 1975]

Large-λ asymptotic expansion for the integral

$$\int_K \mathrm{d}^N x\, \mu(x) e^{\lambda S(r,x)} = \left(\frac{1}{\lambda}\right)^{\frac{N}{2}} \frac{e^{\lambda \mathcal{S}(r,Z(r))} \mu(Z(r))}{\sqrt{\det\left(-\delta^2_{z,z} \mathcal{S}(r,Z(r))/2\pi\right)}} [1 + O(1/\lambda)]$$

- The dominant contribution from the complex critical point.

Complex Critical Points

[Hörmander, 1983; Melin, Sjöstrand, 1975]

Large-λ asymptotic expansion for the integral

$$\int_K \mathrm{d}^N x\, \mu(x) e^{\lambda S(r,x)} = \left(\frac{1}{\lambda}\right)^{\frac{N}{2}} \frac{e^{\lambda \mathcal{S}(r,Z(r))}\mu(Z(r))}{\sqrt{\det\left(-\delta^2_{z,z}\mathcal{S}(r,Z(r))/2\pi\right)}}\left[1+O(1/\lambda)\right]$$

- The dominant contribution from the complex critical point.
- Interpolating two regimes:

$$\begin{cases} r=\mathring{r}, & \mathrm{Re}(\mathcal{S}(\mathring{r},Z(\mathring{r}))=0, & \text{power-law decay.} \\ r\neq\mathring{r}, & \mathrm{Re}(\mathcal{S}(r,Z(r))<0, & \text{damping factor } e^{\lambda \mathrm{Re}(\mathcal{S})} \end{cases}$$

- $\frac{1}{\lambda}$ is a *finite* expansion parameter, like $\hbar$ in quantum mechanics.

Complex Critical Points

[Hörmander, 1983; Melin, Sjöstrand, 1975]

Large-λ asymptotic expansion for the integral

$$\int_K \mathrm{d}^N x\, \mu(x) e^{\lambda S(r,x)} = \left(\frac{1}{\lambda}\right)^{\frac{N}{2}} \frac{e^{\lambda \mathcal{S}(r,Z(r))}\mu(Z(r))}{\sqrt{\det\left(-\delta^2_{z,z}\mathcal{S}(r,Z(r))/2\pi\right)}}\left[1+O(1/\lambda)\right]$$

- The dominant contribution from the complex critical point.
- Interpolating two regimes:

$$\begin{cases} r=\mathring{r}, & \mathrm{Re}(\mathcal{S}(\mathring{r},Z(\mathring{r}))=0, & \text{power-law decay.} \\ r\neq\mathring{r}, & \mathrm{Re}(\mathcal{S}(r,Z(r))<0, & \text{damping factor } e^{\lambda \mathrm{Re}(\mathcal{S})} \end{cases}$$

- $\frac{1}{\lambda}$ is a *finite* expansion parameter, like $\hbar$ in quantum mechanics.
- Given any λ, $e^{\lambda \mathrm{Re}(\mathcal{S})}$ may not be small, e.g. $e^{\lambda \mathrm{Re}(\mathcal{S})} = e^{-1}$ if $\mathrm{Re}(\mathcal{S}) = -1/\lambda$.

Outline

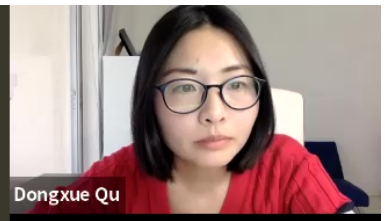

Δ_3 triangulation

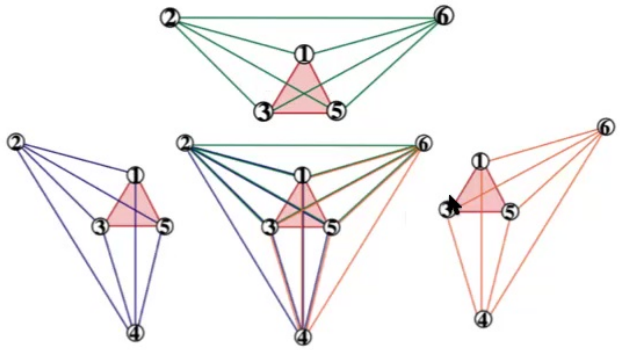

- Δ_3 contains three 4-simplices and a single internal face h.
- All edges are on the boundary, boundary edges-lengths determine Regge geometry on Δ_3.
- $r = \{j_b, \xi_{eb}\}$ is the boundary data, determining boundary edge-lengths, and Regge geometry $\mathbf{g}(r)$.
- All tetrahedra and triangles are spacelike.

Algorithm of $A(\Delta_3)$

We numerically construct boundary data, flat geometry, and real critical point.

$\zeta_{a,b}$ \ b / a	1	2	3	4	5
1	\	(1.,0.01 + 0.01i)	(0.87,0.01+0.49i)	(0.87,0.46+0.17i)	(0.3, -0.55-0.78i)
2	(1.-0.01,-0.01i)	\	(0.49,0.02+0.87i)	(0.49,0.82+0.31i)	(0.95,-0.17-0.25i)
3	(0.86,-0.01+0.51i)	(0.51,-0.02+0.86i)	\	(0.71,0.56-0.43i)	(0.71,-0.24+0.67i)
4	(0.86,0.48+0.16i)	(0.51,0.82+0.27i)	(0.71,0.59-0.39i)	\	**(0.71, 0.71)**
5	(0.3,-0.55-0.78i)	(0.95,-0.17-0.25i)	(0.71,-0.24+0.67i)	**(0.71, 0.71)**	\

a	1	2	3
$\hat{g}_a$	$\begin{pmatrix} 1.16 & 0.06-0.09i \\ 0.06+0.09i & 0.87 \end{pmatrix}$	$\begin{pmatrix} 0.87 & 0.06-0.09i \\ 0.06+0.09i & 1.16 \end{pmatrix}$	$\begin{pmatrix} 1.02 & 0.06+0.17i \\ 0.06-0.17i & 1.02 \end{pmatrix}$
a	4	5	
$\hat{g}_a$	$\begin{pmatrix} 1.03 & 0 \\ -0.36 & 0.97 \end{pmatrix}$	$\begin{pmatrix} 1 & 0 \\ 0 & 1 \end{pmatrix}$	

$\zeta_{a,b}$ \ b / a	6	7	8	9	10
6	\	(0.95,-0.17-0.25i)	**(0.71, 0.71)**	(0.71,-0.24+0.67i)	(0.3,-0.55-0.78i)
7	(0.95,-0.17-0.25i)	\	(0.29,-0.47+0.83i)	(0.88,-0.02-0.48i)	(1.,-0.02-0.03i)
8	**(0.71, 0.71)**	(0.31,-0.57+0.76i)	\	(0.71,0.25+0.66i)	(0.31,0.57-0.76i)
9	(0.71,-0.24+0.67i)	(0.85,0.02-0.52i)	(0.71,0.19+0.68i)	\	(0.85,-0.02+0.52i)
10	(0.3,-0.55-0.78i)	(1.0.02+0.03i)	(0.29,0.47-0.83i)	(0.88,0.02+0.48i)	\

a	6	7	8
$\hat{g}_a$	$\begin{pmatrix} 1 & 0 \\ 0 & 1 \end{pmatrix}$	$\begin{pmatrix} 1.26 & -0.09+0.13i \\ -0.09-0.13i & 0.82 \end{pmatrix}$	$\begin{pmatrix} 0.97 & -0.34 \\ 0 & 1.03 \end{pmatrix}$
a	9	10	
$\hat{g}_a$	$\begin{pmatrix} 1.04 & -0.09-0.25i \\ -0.09+0.25i & 1.04 \end{pmatrix}$	$\begin{pmatrix} 0.82 & -0.09+0.13i \\ -0.09-0.13i & 1.26 \end{pmatrix}$	

$\zeta_{a,b}$ \ b / a	11	12	13	14	15
11	\	**(0.71, 0.71)**	(0.31,-0.57+0.76i)	(0.71,0.25+0.66i)	(0.31,0.57-0.76i)
12	**(0.71, 0.71)**	\	(0.51,0.82+0.27i)	(0.71,0.59-0.39i)	(0.86,0.48+0.16i)
13	(0.31,-0.57+0.76i)	(0.51,0.82+0.27i)	\	(0.5,0.871i)	(0.0.95+0.31i)
14	(0.71,0.25+0.66i)	(0.71,0.59-0.39i)	(0.5,0.871i)	\	(0.5,-0.871i)
15	(0.31,0.57-0.76i)	(0.86,0.48+0.16i)	(0,-0.95-0.31i)	(0.5,-0.871i)	\

a	11	12	13
$\hat{g}_a$	$\begin{pmatrix} 1.04 & 0.02 \\ 0.36 & 0.97 \end{pmatrix}$	$\begin{pmatrix} 0.97 & 0.36 \\ 0 & 1.03 \end{pmatrix}$	$\begin{pmatrix} 1.02+0.0005i & 0.19-0.003i \\ 0.19+0.003i & 1.01-0.0005i \end{pmatrix}$
a	14	15	
$\hat{g}_a$	$\begin{pmatrix} 1.02-0.001i & 0.19+0.006i \\ 0.19-0.006i & 1.02+0.001i \end{pmatrix}$	$\begin{pmatrix} 1.02+0.0005i & 0.19-0.003i \\ 0.19+0.003i & 1.01-0.0005i \end{pmatrix}$	

area $j_{a,b}$ \ b / b	2	3	4	5
1	2	2	2	5
2	\	2	2	5
3	\	\	2	5
4	\	\	\	**5**

area $j_{a,b}$ \ b / b	7	8	9	10
6	5	**5**	5	5
7	\	4.71	5.19	5.19
8	\	\	4.71	4.71
9	\	\	\	5.19

area $j_{a,b}$ \ b / a	12	13	14	15
11	**5**	4.71	4.71	4.71
12	\	2	2	2
13	\	\	3.18	3.18
14	\	\	\	3.18

$\lvert z_{a,b} \rvert$ \ b / a	2	3	4	5
1	(1,0.06 + 0.08i)	(1,0.07 + 0.47i)	(1,0.42 + 0.22i)	(1,-1.82 - 2.57i)
2	\	(1,0.31 + 2.08i)	(1,1.86 + 0.99i)	(1,-0.18 - 0.26i)
3	\	\	(1,0.68 - 0.73i)	(1,-0.33 + 0.94i)
4	\	\	\	(1,1)

Algorithm of $A(\Delta_3)$

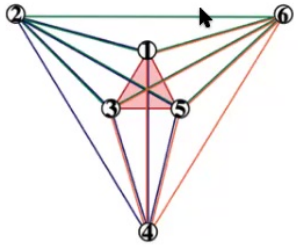

- We vary the length l_{26}. It gives a family of boundary data $r = \mathring{r} + \delta r$. We obtain numerically a family of curved geometries $\mathbf{g}(r)$:

$$\begin{aligned} \text{Length variation } \delta l_{26}: &\quad 0.7 \times 10^{-12} \sim 10^{-4} \\ \text{Deficit angle } \delta_h: &\quad 1.4 \times 10^{-12} \sim 0.0002 \end{aligned}$$

- For each $\delta_h \neq 0$, the real critical point is absent.
- Numerically compute the complex critical point $z = Z(r)$ satisfying $\partial_z \mathcal{S}(r, z) = 0$ with Newton-like recursive procedure:

Algorithm of $A(\Delta_3)$

1. We linearize $\partial_z \mathcal{S}(r,z)=0$ at $x_0 \in \mathbb{R}^{124}$ (satisfying $\mathrm{Re}(S)=\partial_g S=\partial_{\mathbf{z}} S=0$, but $\partial_{j_h} S \neq 0$)

$$\partial_z \mathcal{S}(r,x_0)+\partial_z^2 \mathcal{S}(r,x_0)\cdot \delta z_1=0,$$

   the solution is $z_1=x_0+\delta z_1$.
2. Similarly, we linearize $\partial_z \mathcal{S}(r,z)=0$ at z_1, the solution is $z_2=z_1+\delta z_2$.
3. We linearize $\partial_z \mathcal{S}(r,z)=0$ at z_2, $\cdots\cdots$
4. $\cdots\cdots$
5. We linearize $\partial_z \mathcal{S}(r,z)=0$ at z_{n-1}, the solution approximates the complex critical point $Z(r)\simeq z_n=z_{n-1}+\delta z_n$.
6. Practically, we use $n=4$.
7. Absolute Error: $\varepsilon=\max|\partial_z \mathcal{S}(r,z_n)|\approx 1.31\delta_h^5$.

δ_h	2×10^{-16}	2×10^{-12}	3×10^{-8}	6×10^{-6}	4×10^{-5}	2×10^{-4}
ε	2×10^{-79}	4.27×10^{-59}	3.19×10^{-38}	1.02×10^{-26}	1.34×10^{-22}	4.2×10^{-19}

Numerical Results

We numerically compute the complex critical point $Z(r)$ for many r corresponding to curved geometries.

We compute numerically $\mathcal{S}$ and the difference $\delta\mathcal{I}(r)$ from the Regge action of the curved geometry $\mathbf{g}(r)$:

$$\mathcal{S}(r, Z(r)) = i\mathcal{I}_R[\mathbf{g}(r)] + \delta\mathcal{I}(r), \quad \mathcal{I}_R[\mathbf{g}(r)] = \mathfrak{a}_h(r)\delta_h(r) + \sum_b \mathfrak{a}_b(r)\Theta_b(r).$$

At $\lambda = 10^{11}, \gamma = 0.1$,

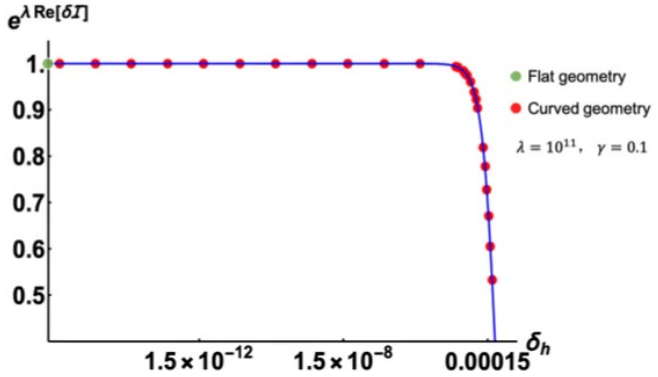

Numerical Results

We numerically fit $e^{\lambda \mathrm{Re}(\delta\mathcal{I})}$ (blue curve) and $e^{i\lambda \mathrm{Im}(\delta\mathcal{I})}$

$$\delta\mathcal{I} = a_2\delta_h^2 + a_3\delta_h^3 + a_4\delta_h^4 + O(\delta_h^5)$$

The best fit coefficient a_i and the corresponding fitting errors at $\gamma = 0.1$ are

$$\begin{aligned} a_2 &= -0.00016_{\pm 10^{-17}} - i0.00083_{\pm 10^{-16}}, \\ a_3 &= -0.0071_{\pm 10^{-13}} - i0.011_{\pm 10^{-12}}, \\ a_4 &= -0.059_{\pm 10^{-9}} + i0.070_{\pm 10^{-8}}. \end{aligned}$$

The effective action $\mathcal{S}$ is the Regge action plus "high curvature correction":

$$\mathcal{S}(r, Z(r)) = i\mathcal{I}_R[\mathbf{g}(r)] + \delta\mathcal{I}(r),$$

Large-λ asymptotic expansion for the integral

$$\int_K \mathrm{d}^N x\, \mu(x) e^{\lambda S(r,x)} = \left(\frac{1}{\lambda}\right)^{\frac{N}{2}} \frac{e^{\lambda \mathcal{S}(r,Z(r))}\mu(Z(r))}{\sqrt{\det\left(-\delta^2_{z,z}\mathcal{S}(r,Z(r))/2\pi\right)}} [1 + O(1/\lambda)]$$

Numerical Results

The contour plots of $e^{\lambda \mathrm{Re}[\delta \mathcal{I}(r)]} \propto |A(\Delta_3)|$:

$\gamma = 0.1$ $\qquad$ $\lambda = 5 \times 10^{10}$

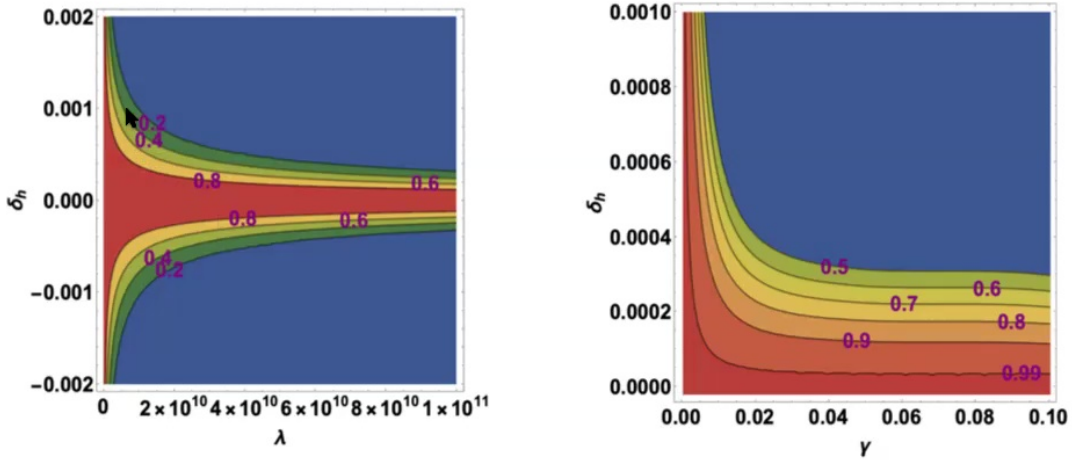

The non-blue regime of curved geometries where $A(\Delta_3)$ is not small.

Cosine Problem

Natively,

$$\begin{aligned} A(\Delta_3^{\mathbf{I}}) &\sim (e^{i\mathcal{I}_R} + e^{-i\mathcal{I}_R})(e^{i\mathcal{I}_R} + e^{-i\mathcal{I}_R})(e^{i\mathcal{I}_R} + e^{-i\mathcal{I}_R}) \\ &= 8 \text{ terms} \end{aligned}$$

- 8 terms correspond to 2 continuous 4-simplex orientations

$$+++, \quad ---$$

and 6 discontinuous 4-simplex orientations:

$$++-, \quad +--, \quad --+, \quad -+-, \quad +-+, \quad -++,$$

Cosine Problem

- Flatness constraint changes to:

$$\gamma\delta_h^s = \gamma \sum_{v\in h} s_v \Theta_h(v) = 0 \mod 4\pi\mathbb{Z},$$

$s_v = \pm$ are opposite orientations at the 4-simplex v.

- Given the boundary data $\mathring{r}$,

s	$+++$	$---$	$++-$	$--+$	$+--$	$-++$	$-+-$	$+-+$
δ_h^s	0	0	0.043	−0.043	0.72	−0.72	−0.68	0.68

there are only 2 real critical points with all $s_v = +$ or $s_v = -$.

Asymptotics of $A(\Delta_3)$

- With $r = \mathring{r} + \delta r$ of curved geometries $\mathbf{g}(r)$

$$A(\Delta_3) \sim \left(\frac{1}{\lambda}\right)^{60} \left[\mathscr{N}_+ e^{i\lambda \mathcal{I}_R[\mathbf{g}(r)]+\lambda\delta\mathcal{I}(r)} + \mathscr{N}_- e^{-i\lambda \mathcal{I}_R[\mathbf{g}(r)]+\lambda\delta\mathcal{I}'(r)}\right]$$

contributed by the complex critical points close to these 24 real critical points.

Cosine problem is relaxed in this example.

$$\begin{aligned}
\text{Regge action: } \mathcal{I}_R &= \mathfrak{a}_h \delta_h + \sum_b \mathfrak{a}_b \Theta_b, \\
\text{High curvature correction: } \delta\mathcal{I} &= a_2\delta_h^2 + a_3\delta_h^3 + a_4\delta_h^4 + O(\delta_h^5), \\
\delta\mathcal{I}' &= \bar{a}_2\delta_h^2 - \bar{a}_3\delta_h^3 + \bar{a}_4\delta_h^4 + O(\delta_h^5)
\end{aligned}$$

Outline

1. Motivation and Results
2. EPRL Spinfoam Model
3. Real and Complex critical points
4. Numerical Implementation: Δ_3
5. Numerical Implementation: 1-5 Pachner Move

1-5 Pachner move

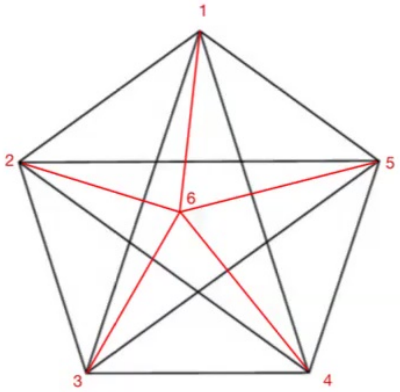

- σ_{1-5}: the complex of the 1-5 Pachner move refining a 4-simplex into five 4-simplices.
- Simplicial complex: 1 internal site, 5 internal segments (red), 10 boundary triangles b, and 10 internal triangles h.

$$A(\sigma_{1\text{-}5}) = \int \mathrm{d}j_{12}\mathrm{d}j_{13}\mathrm{d}j_{14}\mathrm{d}j_{15}\mathrm{d}j_{23}\, \mathcal{Z}_{\sigma_{1\text{-}5}}\left(j_{12}, j_{13}, j_{14}, j_{15}, j_{23}\right),$$

$$\mathcal{Z}_{\sigma_{1\text{-}5}} = \sum_{\{k_h\}} \int \prod_{\bar{h}=1}^{5} \mathrm{d}j_{\bar{h}} \prod_{h=1}^{10} (2\lambda) d_{\lambda j_h} \int [\mathrm{d}g\mathrm{d}\mathbf{z}] e^{\lambda S^{(k)}},$$

1-5 Pachner move

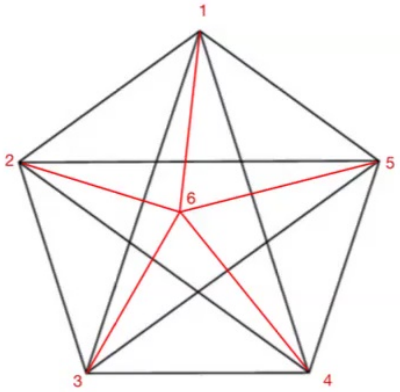

- σ_{1-5}: the complex of the 1-5 Pachner move refining a 4-simplex into five 4-simplices.
- Simplicial complex: 1 internal site, 5 internal segments (red), 10 boundary triangles b, and 10 internal triangles h.
- Regge geometries $\mathbf{g}(r)$ are determined by the boundary data and five lengths $l_{m6}, m = 1, 2, 3, 4, 5$.
- Locally change variables (Heron's formula): $l_{m6} \to j_{12}, j_{13}, j_{14}, j_{15}, j_{23}$.

$$A(\sigma_{1\text{-}5}) = \int \mathrm{d}j_{12}\mathrm{d}j_{13}\mathrm{d}j_{14}\mathrm{d}j_{15}\mathrm{d}j_{23}\, \mathcal{Z}_{\sigma_{1\text{-}5}}\left(j_{12}, j_{13}, j_{14}, j_{15}, j_{23}\right),$$

$$\mathcal{Z}_{\sigma_{1\text{-}5}} = \sum_{\{k_h\}} \int \prod_{\bar{h}=1}^{5} \mathrm{d}j_{\bar{h}} \prod_{h=1}^{10} (2\lambda) d_{\lambda j_h} \int [\mathrm{d}g\mathrm{d}\mathbf{z}] e^{\lambda S^{(k)}},$$

1-5 Pachner move

$$A(\sigma_{1\text{-}5}) = \int \mathrm{d}j_{12}\mathrm{d}j_{13}\mathrm{d}j_{14}\mathrm{d}j_{15}\mathrm{d}j_{23}\, \mathcal{Z}_{\sigma_{1\text{-}5}}(j_{12}, j_{13}, j_{14}, j_{15}, j_{23})$$

$$\mathcal{Z}_{\sigma_{1\text{-}5}} = \sum_{\{k_h\}} \int \prod_{\bar{h}=1}^{5} \mathrm{d}j_{\bar{h}} \prod_{h=1}^{10} (2\lambda) d_{\lambda j_h} \int [\mathrm{d}g\mathrm{d}\mathbf{z}] e^{\lambda S^{(k)}},$$

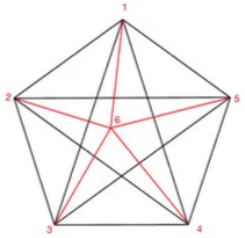

- We focus on the 195-dim integral in $\mathcal{Z}_{\sigma_{1\text{-}5}}$ with $k_h = 0$.
- For $\mathcal{Z}_{\sigma_{1\text{-}5}}$, the external parameters: $r \triangleq \{j_{12}, j_{13}, j_{14}, j_{15}, j_{23}; j_b, \xi_{eb}\}$. $\mathring{r}$ determines the flat geometry $\mathbf{g}(\mathring{r})$, and the (non-degenerate) real critical point $\{\mathring{j}_{\bar{h}}, \mathring{g}_{ve}, \mathring{\mathbf{z}}_{vf}\}$ with all $s_v = +$.
- Fixing $\mathring{j}_b, \mathring{\xi}_{eb}$, we deform $l_{m6} = \mathring{l}_{m6} + \delta l_{m6}$, so that e.g. $j_{12} = \mathring{j}_{12} + \delta j_{12}, \cdots$, and $r = \mathring{r} + \delta r$ with random sampling.

1-5 Pachner move

$$A(\sigma_{1\text{-}5}) = \int \mathrm{d}j_{12}\mathrm{d}j_{13}\mathrm{d}j_{14}\mathrm{d}j_{15}\mathrm{d}j_{23}\, \mathcal{Z}_{\sigma_{1\text{-}5}}(j_{12}, j_{13}, j_{14}, j_{15}, j_{23})$$

$$\mathcal{Z}_{\sigma_{1\text{-}5}} = \sum_{\{k_h\}} \int \prod_{\bar{h}=1}^{5} \mathrm{d}j_{\bar{h}} \prod_{h=1}^{10} (2\lambda) d_{\lambda j_h} \int [\mathrm{d}g\mathrm{d}\mathbf{z}] e^{\lambda S^{(k)}},$$

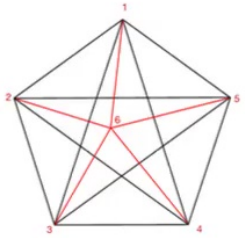

- We focus on the 195-dim integral in $\mathcal{Z}_{\sigma_{1\text{-}5}}$ with $k_h = 0$.
- For $\mathcal{Z}_{\sigma_{1\text{-}5}}$, the external parameters: $r = \{j_{12}, j_{13}, j_{14}, j_{15}, j_{23}; j_b, \xi_{eb}\}$. $\mathring{r}$ determines the flat geometry $\mathbf{g}(\mathring{r})$, and the (non-degenerate) real critical point $\{\mathring{j}_{\bar{h}}, \mathring{g}_{ve}, \mathring{\mathbf{z}}_{vf}\}$ with all $s_v = +$.
- Fixing $\mathring{j}_b, \mathring{\xi}_{eb}$, we deform $l_{m6} = \mathring{l}_{m6} + \delta l_{m6}$, so that e.g. $j_{12} = \mathring{j}_{12} + \delta j_{12}, \cdots$, and $r = \mathring{r} + \delta r$ with random sampling.
- There is 1 DoF $r = \mathring{r} + \delta r$. $\mathbf{g}(r)$ are curved geometries with small deficit angles $< 10^{-3}$. The real critical point is absent.

- Compute numerically complex critical points $Z(r)$ for many r.
- $\mathcal{S}(r, Z(r)) = i\mathcal{I}_R[\mathbf{g}(r)] + \delta\mathcal{I}(r)$,

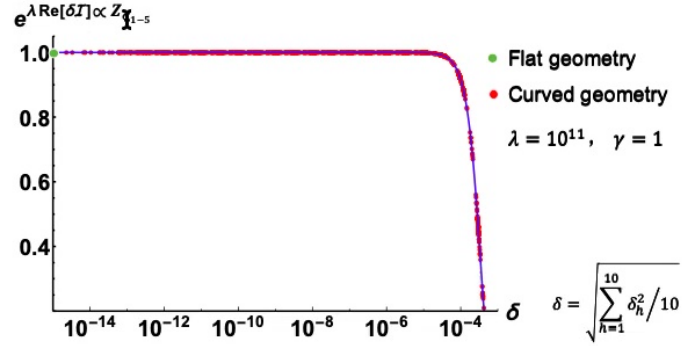

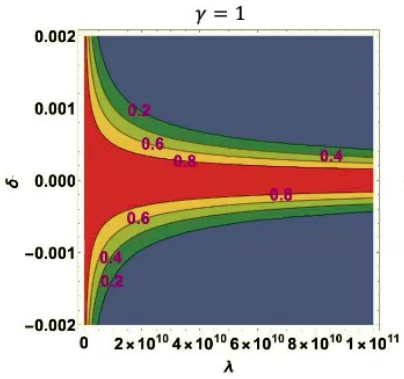

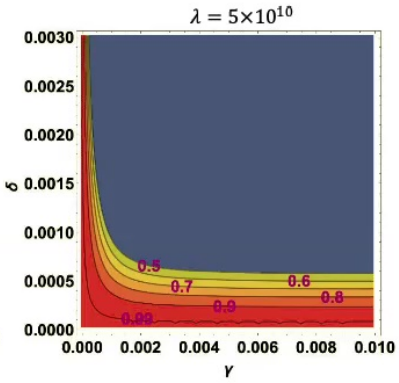

1-5 Pachner move

$$A(\sigma_{1\text{-}5}) \quad = \quad \int \mathrm{d}j_{12}\mathrm{d}j_{13}\mathrm{d}j_{14}\mathrm{d}j_{15}\mathrm{d}j_{23}\, \mathcal{Z}_{\sigma_{1\text{-}5}}\left(j_{12}, j_{13}, j_{14}, j_{15}, j_{23}\right),$$

Insert the asymptotic expansion of $\mathcal{Z}_{\sigma_{1\text{-}5}}$ back in $A(\sigma_{1\text{-}5})$, we obtain integral over Regge geometries:

$$\left(\frac{1}{\lambda}\right)^{\frac{N}{2}} \int_{\mathbf{I}} \prod_{m=1}^{5} \mathrm{d}l_{m6}\, e^{\lambda \mathcal{S}(r, Z(r))} \mathscr{N}_r \left[1 + O(1/\lambda)\right],$$

we have changed $\mathrm{d}j \to \mathrm{d}l$ and $r = r(l)$.

The action is Regge action plus "high curvature correction":

$$\mathcal{S}(r, Z(r)) = i\mathcal{I}_R[\mathbf{g}(r)] - a(\gamma)\delta(r)^2 + O(\delta^3),$$

$\gamma = 1$, $a = 8.88 \times 10^{-5}_{\pm 10^{-12}} - i0.033_{\pm 10^{-10}}$.

For small γ and δ, $\left|e^{\lambda \mathcal{S}}\right| \sim O(1) \Longleftrightarrow \gamma^2\delta^2 < \frac{1}{\lambda}$

[Asante, Dittrich, Haggard, 2020; Han, 2013]

Summary

- EPRL spinfoam amplitudes allow curved Regge geometries with small deficit angles.
- The curved geometries correspond to complex critical points that are slightly away from the real integration domain.
- Regge geometries with small deficit angles are sufficient for approximating arbitrary smooth curved geometry.
- The dominant contribution to the spinfoam amplitude is proportional to $e^{\mathcal{S}}$, $\mathcal{S}$ is the Regge action of the curved geometry plus the curvature correction of order δ_h^2 and higher.

$$\mathcal{S} = i\mathcal{I}_R[\mathbf{g}(r)] + a_2\delta_h^2 + a_3\delta_h^3 + a_4\delta_h^4 + O(\delta_h^5),$$

- Δ_3: relaxing cosine problem.
- 1-5 Pachner move: reduce the spinfoam amplitude to integral over Regge geometries:

$$\left(\frac{1}{\lambda}\right)^{\frac{N}{2}} \int \prod_{m=1}^{5} \mathrm{d}l_{m6}\, e^{\lambda \mathcal{S}(r,Z(r))} \mathscr{N}_r \left[1 + O(1/\lambda)\right].$$

Outlook

- Compare with effective spinfoam model.
- Observables, e.g., correlation functions.
- More complicated complex.
- Lattice Refinement.
- Larger deficit angles and higher order correction.
- ...

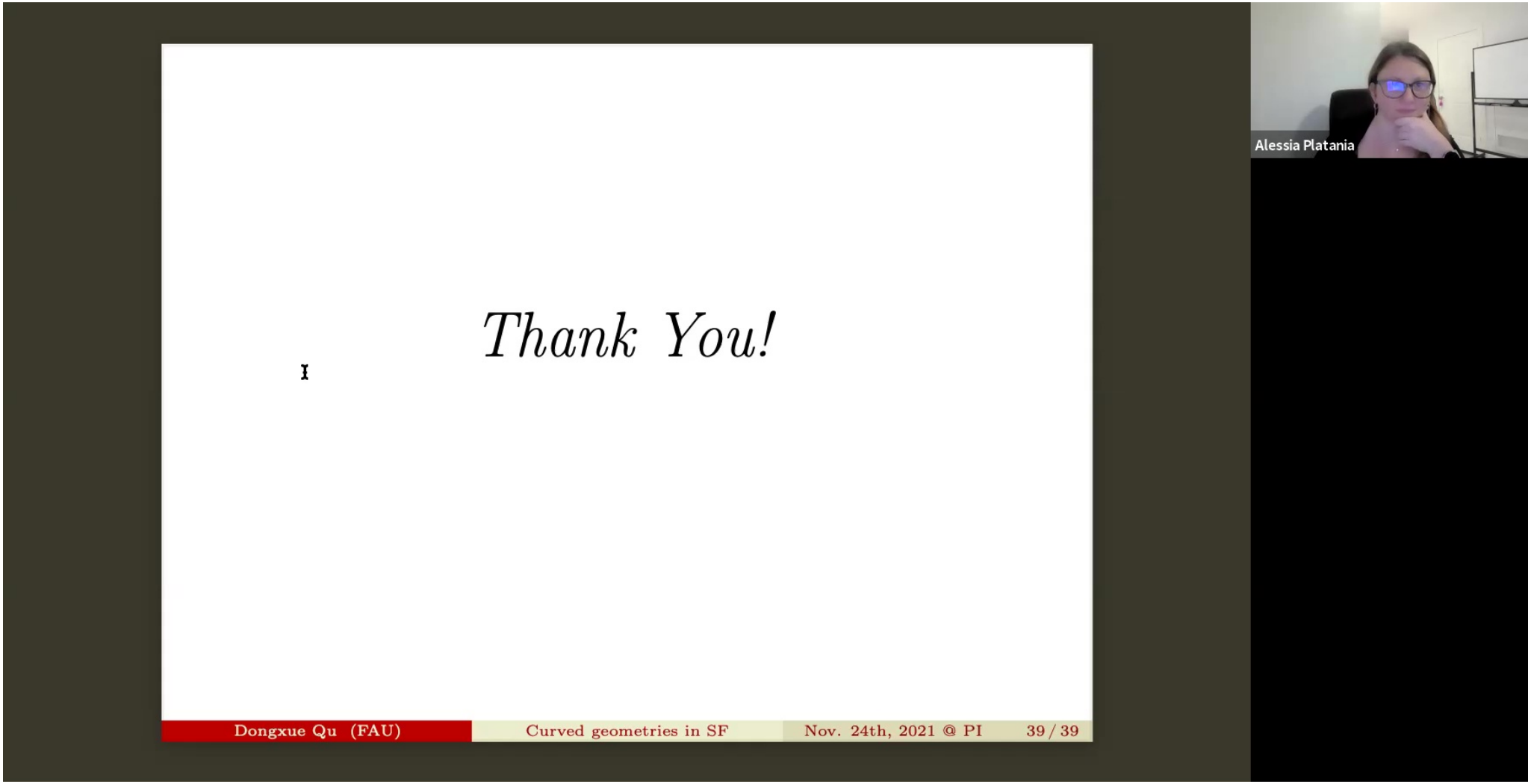
Thank You!
Dongxue Qu (FAU)
Curved geometries in SF
Nov. 24th, 2021 @ PI
39 / 39
Alessia Platania